Journal of Applied Fluid Mechanics, Vol. 9, No. 3, pp. 1329-1337, 2016.
Available online at www.jafmonline.net, ISSN 1735-3572, EISSN 1735-3645.
DOI: 10.18869/acadpub.jafm.68.228.24685

Flow of an Oldroyd-B Fluid past an Unsteady Bidirectional Stretching Sheet with Constant Temperature and Constant Heat Flux

M. Ahmad[1†], I. Ahmad[1], M. Sajid[2,3] and A. Abbasi[1]

[1]*Department of Mathematics, University of Azad Jammu & Kashmir, Muzaffarabad 13100, Pakistan*
[2]*Theoretical Physics Division, PINSTECH, P.O. Nilore, Islamabad 44000, Pakistan*
[3]*AS-ICTP, Strada Costiera 11, Trieste, Italy*

†*Corresponding Author Email: manzoorajku@gmail.com*

(Received February 7, 2015; accepted July 13, 2015)

ABSTRACT

This article describes the time dependent flow of a non-Newtonian fluid with heat transfer. We consider three dimensional unsteady flow and heat transfer of an Oldroyd-B fluid for constant temperature (CT) and constant heat flux (CH) cases over an unsteady bidirectional stretching surface. Homotopic solutions of the governing boundary value problems have been computed. Convergence for both velocity and temperature profiles is explored. The effects of emerging parameters on the velocity and temperature fields are investigated with the help of graphs and tabular data. It is observed that due to unsteadiness temperature in both the constant temperature and constant heat flux cases decrease significantly. Comparison of obtained and previously published results is found in excellent agreement.

Keywords: Unsteady flow; Bidirectional stretching; Oldroyd-B fluid; Heat transfer analysis; Homotopy analysis method.

NOMENCLATURE

A	unsteadiness parameter	ν	kinematic viscosity
C_p	specific heat	x, y, z	Cartesian coordinates
$C_1 - C_{10}$	integration constants.		
f, g	dimensionless velocities	θ, ϕ	dimensionless temperatures
$\hbar_f, \hbar_g, \hbar_\theta, \hbar_\phi$	auxiliary parameters	η	dimensionless independent varialbe
k	thermal conductivity	α	stretching ratio
k_1	thermal conductivity	β	internal heat parameter
Pr	Prandtl number	β_1	relaxation parameter
p	embedding parameter	β_2	retardation parameter
Q	heat source or sink	ρ	fluid density
r, s	power indices		

1. INTRODUCTION

The key importance of non-Newtonian fluids in industry and technology attracted many researchers. The constitutive relationships of non-Newtonian fluids are nonlinear and can predict different phenomena like shear thinning, shear thickening, normal stress effects, stress relaxation, retardation and fluid memory etc. Different nature of phenomena cannot be described by a single constitutive relationship between the shear stress and rate of deformation. Hence, different constitutive models of such fluids have been proposed in the literature. An Oldroyd-B fluid is in the subclass of rate type non-Newtonian fluids which exhibit both relaxation and retardation effects as discussed by Haitao and Mingyu (2009), Sajid *et al*. (2010), Jamil *et al*. (2011), Liu *et al*. (2011), Hayat *et al*. (2011), Hayat *et al*. (2012), Hayat *et al*. (2014), Shehzad *et al*. (2014), Khan *et al*. (2014).

The pioneering problem for two dimensional boundary layer flow due to a stretching plane surface discussed by Crane (1970) is involved in many manufacturing process such as glass fiber production, hot rolling, continuous casting, manufacturing of sheets, coating and paper production. The three-dimensional flow due to a plane bidirectional linearly stretching sheet was first

discussed by Wang (1989). He found an exact numerical solution of classical Navier-Stokes equations. Ariel (2003) derived approximate analytic and numerical solutions for the steady three dimensional flows over a stretching sheet. Liu and Andersson (2008) considered the heat transfer in three dimensional flow due to a non-isothermal stretching sheet. Ahmad *et al*. (2011) extended the problem carried out by Liu and Andersson (2008) by incorporating the effects of applied magnetic field and Darcy resistane.

A literature survey sheds light on the fact that only few studies have been reported on the problem of unsteady boundary layer flows due to a stretching sheet. Xu *et al*. (2007) examined uniformly valid series solutions for three dimensional unsteady flow caused by an impulsive stretching sheet. The unsteady three dimensional flow and mass transfer of elastico-viscous fluid due to unsteady stretching sheet with constant wall concentration was studied by Hayat *et al*. (2011). Recently Awais *et al*. (2014) studied time dependent boundary layer flow of a Maxwell fluid over an unsteady bidirectional stretching sheet. Very recently Ahmad *et al*. (2014) discussed heat transfer analysis of MHD flow due to unsteady bidirectional stretching sheet through porous space. To the best of our knowledge, the analysis for the three-dimensional unsteady flow of an Oldroyd-B fluid over an unsteady bidirectional stretching surface with heat transfer has not yet been reported in the literature.

The purpose of present communication is to discuss the simultaneous effects of heat on the flow of an Oldroyd-B fluid over an unsteady bidirectional stretching surface. The stretching surface exhibits the heat transfer through two cases namely constant temperature (CT) and constant heat flux (CH). Effects of heat generation/absorption are also considered. As a first step the boundary layer equations under these assumptions have been developed and then series solutions by employing a homotopy analysis method (Liao 1992, Liao 2003, Turkyilmazoglu 2012, Ahmad 2013, Hayat *et al*. 2015a, Hayat *et al*. 2015b) are presented for the transformed nonlinear boundary value problems. The effects of various involving physical parameters on the velocity and temperature profiles are discussed through graphs and tables.

2. MATHEMATICAL FORMULATION

Consider the unsteady, three-dimensional, incompressible flow of an Oldroyd-B fluid over an unsteady stretching sheet. The sheet coincides with the plane at $z = 0$ and the fluid occupies the region $z > 0$. Flow analysis is carried out in the presence of heat generation or absorption. Following Haris (1977) the developed boundary layer equations that govern the unsteady flow and heat transfer of an Oldroyd-B fluid are

$$\frac{\partial u}{\partial x}+\frac{\partial v}{\partial y}+\frac{\partial w}{\partial z}=0, \tag{1}$$

$$\frac{\partial u}{\partial t}+u\frac{\partial u}{\partial x}+v\frac{\partial u}{\partial y}+w\frac{\partial u}{\partial z}+$$
$$\lambda_1\left(\begin{array}{l}\frac{\partial^2 u}{\partial t^2}+2u\frac{\partial^2 u}{\partial x\partial t}+2v\frac{\partial^2 u}{\partial y\partial t}+2w\frac{\partial^2 u}{\partial z\partial t}+u^2\frac{\partial^2 u}{\partial x^2}\\ +w^2\frac{\partial^2 u}{\partial z^2}+2uv\frac{\partial^2 u}{\partial x\partial y}+2vw\frac{\partial^2 u}{\partial y\partial z}+2uw\frac{\partial^2 u}{\partial x\partial z}\end{array}\right)=$$
$$\nu\left(\begin{array}{l}\frac{\partial^2 u}{\partial z^2}+\lambda_2\left(\begin{array}{c}\frac{\partial^3 u}{\partial z^2\partial t}+u\frac{\partial^3 u}{\partial x\partial z^2}+v\frac{\partial^3 u}{\partial y\partial z^2}\\ +w\frac{\partial^3 u}{\partial z^3}-\frac{\partial u}{\partial x}\frac{\partial^2 u}{\partial z^2}\\ -\frac{\partial u}{\partial y}\frac{\partial^2 v}{\partial z^2}-\frac{\partial u}{\partial z}\frac{\partial^2 w}{\partial z^2}\end{array}\right)\end{array}\right), \tag{2}$$

$$\frac{\partial v}{\partial t}+u\frac{\partial v}{\partial x}+v\frac{\partial v}{\partial y}+w\frac{\partial v}{\partial z}+$$
$$\lambda_1\left(\begin{array}{l}\frac{\partial^2 v}{\partial t^2}+2u\frac{\partial^2 v}{\partial x\partial t}+2v\frac{\partial^2 v}{\partial y\partial t}+2w\frac{\partial^2 v}{\partial z\partial t}+u^2\frac{\partial^2 v}{\partial x^2}\\ +w^2\frac{\partial^2 v}{\partial z^2}+2uv\frac{\partial^2 v}{\partial x\partial y}+2vw\frac{\partial^2 v}{\partial y\partial z}+2uw\frac{\partial^2 v}{\partial x\partial z}\end{array}\right)=$$
$$\nu\left(\begin{array}{l}\frac{\partial^2 u}{\partial z^2}+\lambda_2\left(\begin{array}{c}\frac{\partial^3 v}{\partial z^2\partial t}+u\frac{\partial^3 v}{\partial x\partial z^2}+v\frac{\partial^3 v}{\partial y\partial z^2}\\ +w\frac{\partial^3 v}{\partial z^3}-\frac{\partial v}{\partial x}\frac{\partial^2 u}{\partial z^2}\\ -\frac{\partial v}{\partial y}\frac{\partial^2 v}{\partial z^2}-\frac{\partial v}{\partial z}\frac{\partial^2 w}{\partial z^2}\end{array}\right)\end{array}\right), \tag{3}$$

$$\frac{\partial T}{\partial t}+u\frac{\partial T}{\partial x}+v\frac{\partial T}{\partial y}+w\frac{\partial T}{\partial z}=k_1\frac{\partial^2 T}{\partial z^2}+\frac{Q}{\rho c_p}(T-T_\infty). \tag{4}$$

The appropriate boundary conditions for the present problem are

$$u=u_w(x),\ \ v=v_w(y),\ \ w=0\ \ \text{at}\ z=0,$$
$$u\to 0,\ \ v\to 0\ \ \text{as}\ \ \ z\to\infty, \tag{5}$$

where

$$u_w(x)=\frac{ax}{1-ct},\ \ v_w(y)=\frac{by}{1-ct},$$

for the temperature we have the following two sets of boundary conditions

(**CT case**):

$$T=T_w=T_\infty+Ax^r y^s\ \text{at z}=0,\ T\to T_\infty\ \text{as}\ z\to\infty, \tag{6}$$

(**CH case**):

$$-\lambda_3\frac{\partial T}{\partial z}=Bx^r y^s\ \ \text{at}\ z=0,\ T\to T_\infty\ \text{as}\ z\to\infty, \tag{7}$$

where $a>0$, $b>0$ and $c>0$ are constant stretching rates with dimension time^{-1} such that $ct<1$, ν is the kinematic viscosity, k_1 is the thermal conductivity of the fluid, λ_1 is the relaxation time, λ_2 is the retardation time, λ_3 is the thermal conductivity of the fluid, T_∞ is the ambient temperature outside the thermal boundary layer, A and B are positive constants. The power indices r and s decided how the temperature or the heat flux at the sheet varies in the (x, y)-plane. The stretching phenomenon in this direction has already studied by various authors Liu and Andersson (2008), Ahmad *et al*. (2011), Ahmad *et al*. (2014).

Following Awais *et al*. (2014) and Ahmad *et al*. (2014), we introduce the following dimensionless variables

$$\eta=\sqrt{\frac{a}{\nu(1-ct)}}z,\ \ u=\frac{ax}{1-ct}f'(\eta),\ \ v=\frac{ay}{1-ct}g'(\eta)$$

$$w = -\sqrt{\frac{a\nu}{1-ct}}\{f(\eta)+g(\eta)\},$$
$$\theta(\eta) = \frac{T(x,y,z,t)-T_\infty}{T_w(x,y)-T_\infty} \text{ for (CT)},$$
$$T(x,y,z,t)-T_\infty = \frac{B}{\lambda_3}\sqrt{\frac{\nu}{a}}x^r y^s \phi(\eta) \text{ for (CH)}. \quad (8)$$

Thus the continuity equation is identically satisfied and Eqs. (2-4) takes the following form

$$f''' - A\left(f' + \frac{\eta}{2}f''\right) - f'^2 + (f+g)f'' - \beta_1\begin{pmatrix}(f+g)^2 f''' - 2(f+g)f'f'' \\ +A^2\left(2f' + \frac{7\eta}{4}f'' + \frac{\eta^2}{4}f'''\right) \\ +A\{2f'^2 + \eta f'f'' - (f+g)(3f'' + \eta f''')\}\end{pmatrix} + \beta_2\left((f''+g'')f'' - (f+g)f'''' + A(\eta f'''' + 2f''')\right), \quad (9)$$

$$g''' - A\left(g' + \frac{\eta}{2}g''\right) - g'^2 + (f+g)g'' - \beta_1\begin{pmatrix}(f+g)^2 g''' - 2(f+g)g'g'' \\ +A^2\left(2g' + \frac{7\eta}{4}g'' + \frac{\eta^2}{4}g'''\right) \\ +A\{2g'^2 + \eta g'g'' - (f+g)(3g'' + \eta g''')\}\end{pmatrix} + \beta_2\left((f''+g'')g'' - (f+g)g'''' + A(\eta g'''' + 2g''')\right), \quad (10)$$

$$\theta'' + Pr(f+g)\theta' + Pr(\beta - rf' - sg')\theta - A\left(\frac{\eta}{2}\theta' - \theta\right)Pr = 0, \quad \text{for (CT)} \quad (11)$$

$$\phi'' + Pr(f+g)\phi' + Pr(\beta - rf' - sg')\phi - A\left(\frac{\eta}{2}\phi' - \phi\right)Pr = 0 \quad \text{for (CH)}. \quad (12)$$

The associated boundary conditions are also reduced into the following form

$$f+g = 0, f' = 1, g' = \alpha, \theta = 1, \phi' = -1 \text{ at } \eta = 0$$
$$f' \to 0,\ g' \to 0,\ \theta \to 0,\ \phi \to 0 \text{ as } \eta \to \infty \quad (13)$$

where the prime denote differentiation with respect to η, $\alpha = b/a$ the stretching ratio, $A = c/a$ the unsteadiness parameter, $\beta_1 = \lambda_1 a/(1-ct)$, $\beta_2 = \lambda_2 a/(1-ct)$ the Deborah numbers, $Pr = \nu/k$ the Prantle number and $\beta = Q/\rho C_p a$ the internal heat generation.

3. HOMOTOPY ANALYSIS SOLUTIONS

Based on the rules of solution expressions and the boundary conditions (13), the initial approximations $f_0(\eta)$, $g_0(\eta)$, $\theta_0(\eta)$ and $\phi_0(\eta)$ for the functions $f(\eta)$, $g(\eta)$, $\theta(\eta)$ and $\phi(\eta)$ are

$$f_0(\eta) = 1 - e^{\eta},$$
$$g_0(\eta) = \alpha(1 - e^{-\eta}),$$
$$\theta_0(\eta) = e^{-\eta},\ \phi_0(\eta) = e^{-\eta}, \quad (14)$$

and the auxiliary linear operators are

$$\mathcal{L}_1 = f''' - f',\ \mathcal{L}_2 = \theta'' - \theta, \quad (15)$$

satisfying

$$\mathcal{L}_1[C_1 + C_2 e^{\eta} + C_3 e^{-\eta}] = 0,\ \mathcal{L}_2[C_7 e^{\eta} + C_8 e^{-\eta}] = 0, \quad (16)$$

in which $C_i's$ are arbitrary constants. From Eqs. (9)–(12), the nonlinear operators $\mathcal{N}_f, \mathcal{N}_g, \mathcal{N}_\theta$ and $\mathcal{N}_\phi$ are defined by the following expressions

$$\mathcal{N}_f[\hat{f}(\eta,p),\hat{g}(\eta,p)] = \hat{f}'''(\eta,p) - \left(\hat{f}'(\eta,p)\right)^2 + \left(\hat{f}(\eta,p) + \hat{g}(\eta,p)\right)\hat{f}''(\eta,p) - A\left\{\frac{\eta}{2}\hat{f}''(\eta,p) + \hat{f}'(\eta,p)\right\} - \beta_1\begin{Bmatrix}A^2\left\{2\hat{f}'(\eta,p) + \frac{7\eta}{4}\hat{f}''(\eta,p) + \frac{\eta^2}{4}\hat{f}'''(\eta,p)\right\} \\ -A\begin{Bmatrix}2\left(\hat{f}'(\eta,p)\right)^2 + \eta\hat{f}'(\eta,p)\hat{f}''(\eta,p) - \\ \left(\hat{f}(\eta,p) + \hat{g}(\eta,p)\right)\left(3\hat{f}''(\eta,p) + \eta\hat{f}''''(\eta,p)\right)\end{Bmatrix} \\ \begin{Bmatrix}\left(\hat{f}(\eta,p) + \hat{g}(\eta,p)\right)^2\hat{f}'''(\eta,p) - \\ 2\left(\hat{f}(\eta,p) + \hat{g}(\eta,p)\right)\hat{f}'(\eta,p)\hat{f}''(\eta,p)\end{Bmatrix}\end{Bmatrix} + \beta_2\begin{Bmatrix}\left(\hat{f}''(\eta,p) + \hat{g}''(\eta,p)\right)\hat{f}''(\eta,p) \\ -\left(\hat{f}(\eta,p) + \hat{g}(\eta,p)\right)\hat{f}''''(\eta,p) \\ +A\left(\eta\hat{f}''''(\eta,p) + 2\hat{f}'''(\eta,p)\right)\end{Bmatrix}, \quad (17)$$

$$\mathcal{N}_g[\hat{f}(\eta,p),\hat{g}(\eta,p)] = \hat{g}'''(\eta,p) - \left(\hat{g}'(\eta,p)\right)^2 + \left(\hat{f}(\eta,p) + \hat{g}(\eta,p)\right)\hat{g}''(\eta,p) - A\left\{\frac{\eta}{2}\hat{g}''(\eta,p) + \hat{g}'(\eta,p)\right\} - \beta_1\begin{Bmatrix}A^2\left\{2\hat{g}'(\eta,p) + \frac{7\eta}{4}\hat{g}''(\eta,p) + \frac{\eta^2}{4}\hat{g}'''(\eta,p)\right\} \\ -A\begin{Bmatrix}2\left(\hat{g}'(\eta,p)\right)^2 + \eta\hat{g}'(\eta,p)\hat{g}''(\eta,p) - \\ \left(\hat{f}(\eta,p) + \hat{g}(\eta,p)\right)\left(3\hat{g}''(\eta,p) + \eta\hat{g}''''(\eta,p)\right)\end{Bmatrix} \\ \begin{Bmatrix}\left(\hat{f}(\eta,p) + \hat{g}(\eta,p)\right)^2\hat{g}'''(\eta,p) - \\ 2\left(\hat{f}(\eta,p) + \hat{g}(\eta,p)\right)\hat{g}'(\eta,p)\hat{g}''(\eta,p)\end{Bmatrix}\end{Bmatrix} + \beta_2\begin{Bmatrix}\left(\hat{f}''(\eta,p) + \hat{g}''(\eta,p)\right)\hat{g}''(\eta,p) \\ -\left(\hat{f}(\eta,p) + \hat{g}(\eta,p)\right)\hat{g}''''(\eta,p) \\ +A\left(\eta\hat{g}''''(\eta,p) + 2\hat{g}'''(\eta,p)\right)\end{Bmatrix}, \quad (18)$$

$$\mathcal{N}_\theta[\hat{f}(\eta,p),\hat{g}(\eta,p)] = \hat{\theta}''(\eta,p) + Pr\begin{Bmatrix}\left(\hat{f}(\eta,p) + \hat{g}(\eta,p)\right)\hat{\theta}'(\eta,p) \\ +\begin{pmatrix}\beta - r\hat{f}'(\eta,p) \\ -s\hat{g}'(\eta,p)\end{pmatrix}\hat{\theta}(\eta,p) \\ -A\left(\frac{\eta}{2}\hat{\theta}'(\eta,p) + \hat{\theta}(\eta,p)\right)\end{Bmatrix}, \quad (19)$$

$$\mathcal{N}_\phi[\hat{f}(\eta,p),\hat{g}(\eta,p)] = \hat{\phi}''(\eta,p) + Pr\begin{Bmatrix}\left(\hat{f}(\eta,p) + \hat{g}(\eta,p)\right)\hat{\phi}'(\eta,p) \\ +\begin{pmatrix}\beta - r\hat{f}'(\eta,p) \\ -s\hat{g}'(\eta,p)\end{pmatrix}\hat{\phi}(\eta,p) \\ -A\left(\frac{\eta}{2}\hat{\phi}'(\eta,p) + \hat{\phi}(\eta,p)\right)\end{Bmatrix}. \quad (20)$$

If $p \in [0,1]$ is the embedding parameter and $\hbar_f, \hbar_g, \hbar_\theta$ and $\hbar_\phi$ are the non-zero auxiliary parameters, then the zeroth-order deformation problems are of the following form

$$(1-p)\mathcal{L}_1[\hat{f}(\eta,p) - f_0(\eta)] = p\hbar_f\mathcal{N}_f, \quad (21)$$
$$(1-p)\mathcal{L}_1[g(\eta,p) - g_\circ(\eta)] = p\hbar_g\mathcal{N}_g, \quad (22)$$
$$(1-p)\mathcal{L}_2[\hat{\theta}(\eta,p) - \theta_0(\eta)] = p\hbar_\theta\mathcal{N}_\theta, \quad (23)$$
$$(1-p)\mathcal{L}_2[\hat{\phi}(\eta,p) - \phi_0(\eta)] = p\hbar_\phi\mathcal{N}_\phi, \quad (24)$$

$$\hat{f}(0,p) = \hat{g}(0,p) = 0, \quad \hat{f}'(0,p) = \hat{\theta}(0,p) = 1,$$
$$\hat{g}'(0,p) = \alpha,\ \hat{\phi}'(0,p) = -1, \quad (25)$$

Table 1 Numerical values of $f''(0)$, $g''(0)$, $\theta'(0)$ and $\phi''(0)$ at different order of approximations when $\alpha = 0.5$, $\beta_1 = \beta = 0.2$, $\beta_2 = 0.3$, $r = s = 1.0$, $Pr = 1.0$, $\hbar_f = \hbar_g = -0.7$ and $\hbar_\theta = \hbar_\phi = -0.9$.

Order of approximation	$-f''(0)$	$-g''(0)$	$-\theta'(0)$	$\phi''(0)$
1	1.097083	0.482708	1.265000	1.455000
5	1.097084	0.479925	1.445586	1.237031
10	1.097075	0.479903	1.481215	1.210069
15	1.097074	0.479902	1.492032	1.205008
18	1.097074	0.479901	1.494212	1.203597
20	1.097074	0.479901	1.496374	1.202214
25	1.097074	0.479901	1.498309	1.201000
30	1.097074	0.479901	1.498894	1.200639
35	1.097074	0.479901	1.498922	1.200312
40	1.097074	0.479901	1.498922	1.202312

$$\hat{f}'(\infty,p) = \hat{g}'(\infty,p) = \hat{\theta}(\infty,p) = \hat{\phi}(\infty,p) = 0. \tag{26}$$

These equations implies that for $p = 0$ and $p = 1$ have the following solutions

$$\hat{f}(\eta,0) = f_0(\eta)\,,\ \hat{f}(\eta,1) = f(\eta), \tag{27}$$

$$\hat{g}(\eta,0) = g_0(\eta)\,,\ \hat{g}(\eta,1) = g(\eta), \tag{28}$$

$$\hat{\theta}(\eta,0) = \theta_0(\eta)\,,\ \hat{\theta}(\eta,1) = \theta(\eta), \tag{29}$$

$$\hat{\phi}(\eta,0) = \phi_0(\eta)\,,\ \hat{\phi}(\eta,1) = \phi(\eta). \tag{30}$$

$\hat{f}(\eta,p)$, $\hat{g}(\eta,p)$, $\hat{\theta}(\eta,p)$ and $\hat{\phi}(\eta,p)$ varies from $f_0(\eta), g_0(\eta)$, $\theta_0(\eta)$ and $\phi_0(\eta)$ to the solutions $f(\eta)$, $g(\eta)$, $\theta(\eta)$ and $\phi(\eta)$ as p varies from 0 to 1. The Taylor's series thus suggest that

$$\hat{f}(\eta,p) = f_0(\eta) + \sum_{m=1}^{\infty} f_m(\eta)p^m,$$

$$f_m(\eta) = \frac{1}{m!}\frac{\partial^m \hat{f}(\eta,p)}{\partial p^m}\Big|_{p=0}, \tag{31}$$

$$\hat{g}(\eta,p) = g_0(\eta) + \sum_{m=1}^{\infty} g_m(\eta)p^m,$$

$$g_m(\eta) = \frac{1}{m!}\frac{\partial^m \hat{g}(\eta,p)}{\partial p^m}\Big|_{p=0}, \tag{32}$$

$$\hat{\theta}(\eta,p) = \theta_0(\eta) + \sum_{m=1}^{\infty} \theta_m(\eta)p^m,$$

$$\theta_m(\eta) = \frac{1}{m!}\frac{\partial^m \hat{\theta}(\eta,p)}{\partial p^m}\Big|_{p=0}, \tag{33}$$

$$\hat{\phi}(\eta,p) = \phi_0(\eta) + \sum_{m=1}^{\infty} \phi_m(\eta)p^m,$$

$$\phi_m(\eta) = \frac{1}{m!}\frac{\partial^m \hat{\phi}(\eta,p)}{\partial p^m}\Big|_{p=0}, \tag{34}$$

The auxiliary parameters $\hbar_f, \hbar_g, \hbar_\theta$ *and* $\hbar_\phi$ in Eqs. (21)-(24) ensures the the convergence of the series solutions given by Eqs. (31)-(34). Assuming that $\hbar_f, \hbar_g, \hbar_\theta$ *and* $\hbar_\phi$ are chosen such that the series in Eqs. (31)-(34) are convergent at $p = 1$. Thus

$$\hat{f}(\eta) = f_0(\eta) + \sum_{m=1}^{\infty} f_m(\eta), \tag{35}$$

$$\hat{g}(\eta) = g_0(\eta) + \sum_{m=1}^{\infty} g_m(\eta), \tag{36}$$

$$\hat{\theta}(\eta) = \theta_0(\eta) + \sum_{m=1}^{\infty} \theta_m(\eta), \tag{37}$$

$$\hat{\phi}(\eta) = \phi_0(\eta) + \sum_{m=1}^{\infty} \phi_m(\eta). \tag{38}$$

Eqs. (35)-(38) have the general solutions in the forms

$$f_m(\eta) = f_m^*(\eta) + C_1 + C_2 e^{\eta} + C_3 e^{-\eta}, \tag{39}$$

$$g_m(\eta) = g_m^*(\eta) + C_4 + C_5 e^{\eta} + C_6 e^{-\eta}, \tag{40}$$

$$\theta_m(\eta) = \theta_m^*(\eta) + C_7 e^{\eta} + C_8 e^{-\eta}, \tag{41}$$

$$\phi_m(\eta) = \phi_m^*(\eta) + C_9 e^{\eta} + C_{10} e^{-\eta}, \tag{42}$$

where $f_m^*(\eta), g_m^*(\eta), \theta_m^*(\eta)$ and $\phi_m^*(\eta)$ denotes the special solutions.

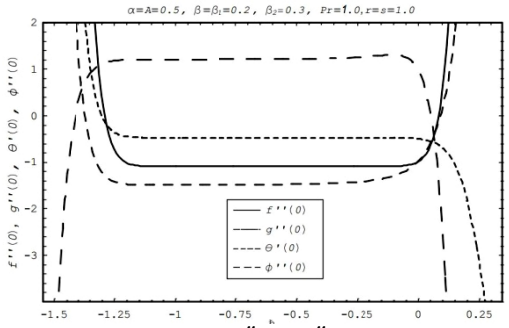

Fig. 1. $\hbar$-curves for $f''(0), g''(0), \theta'(0)$ and $\phi''(0)$ at 18th order of approximation.

4. CONVERGENCE OF THE SERIES SOLUTIONS

The series solutions for f, g, θ and ϕ are given in Eqs. (35)-(38) which contain auxiliary parameters $\hbar_f, \hbar_g$, $\hbar_\theta$ and $\hbar_\phi$. The convergence and rate of approximation of the obtained solutions depends upon these parameters. To find out the suitable values of these auxiliary parameters $\hbar-$ curves for the 18th order of approximation are plotted. Fig. 1 clearly show that the range of admissible values are $-1.20 \le \hbar_f \le -0.1$, $-1.22 \le \hbar_g \le 0$, $-1.22 \le \hbar_\theta \le -0.5$ and $-1.25 \le \hbar_\phi \le -0.5$. Table 1 is made to see that how many order of approximations are required for a convergent solution. It is found

that for velocities f and g 18th order solution is sufficient however for temperatures θ and ϕ the required convergence will be achieved at 35th order of approximation. Hence we need fewer deformations for the velocities as compared to the temperatures for a convergent solution.

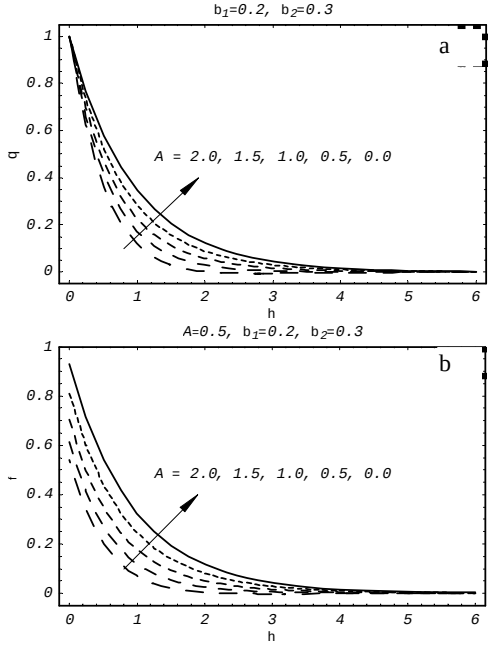

Fig. 2. Influence of unsteadiness parameter *A* on the temperature (a) CT case (b) CH case.

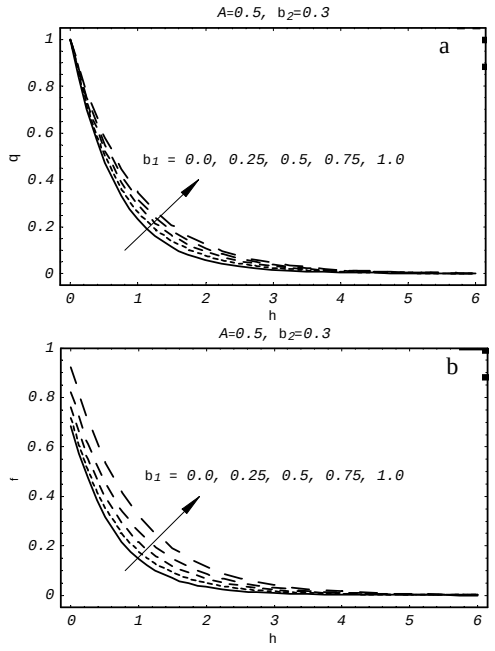

Fig. 3. Influence of Deborah number β_1 on the temperature, (a) CT case (b) CH case.

5. RESULTS AND DISCUSSION

The homotopy analysis method solutions in the form of an infinite series are obtained using symbolic software MATHEMATICA. The values of $\hbar$ are chosen in such a way that the obtained series are convergent for the chosen set of fluid parameters. In the present study we are focusing our attention in the discussion of temperature profiles across the surface for both constant surface temperature and constant heat flux cases. To depict the influence of different parameters on the temperature profiles Figs. 2-9 have been sketched. The influence of parameter A on temperature profiles $\theta(\eta)$ and $\phi(\eta)$ for three dimensional flow situation is portrayed in Fig. 2. This Figure indicates that temperature is a decreasing function of A for both CT and CH cases. It is also noted that the thermal boundary layer thickness decreases with an increase in A. Fig. 3 describes the influence of Deborah number β_1 on the temperature profiles $\theta(\eta)$ and $\phi(\eta)$. It can be seen that as we increase Deborah number β_1 the temperature also increases for both the cases. The deviation of β_2 on $\theta(\eta)$ and $\phi(\eta)$ are seen in Fig. 4. Here we see that the temperature profiles decreases when we increase Deborah number β_2. An increase in Deborah number β_2 is due to increase in retardation time. An increase in retardation time decreases the temperature.

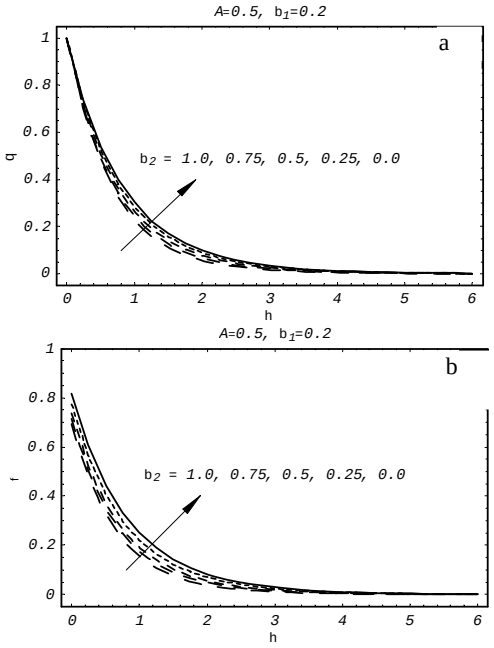

Fig. 4. Influence of Deborah number β_2 on the temperature, (a) CT case (b) CH case.

It is worth mentioning that the stress decreases with an increase in the relaxation parameter. Retardation parameter characterizes the retardation time when strain decreases at constant stress, so velocity decreases by increasing the retardation parameter. A comparison between Figs. 3 and 4 shows that Deborah numbers β_1 and β_2 effects quite oppositely on temperature profiles. Fig. 5 elucidates the influence of stretching ratio α on the temperature profiles. It is noted that the temperature decreases with increasing the stretching ratio α in both CT and CH cases. It is also observed that the thermal boundary layer thickness is decreased for large values of the stretching ratio α. It is further noted that these results are similar in qualitative sense

with the temperature profiles shown by Liu and Andersson (2008).

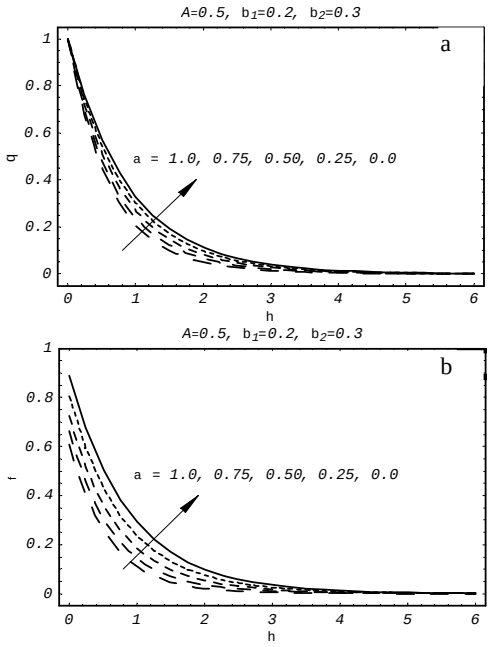

Fig. 5. Influence of stretching parameter α on the temperature, (a) CT case (b) CH case.

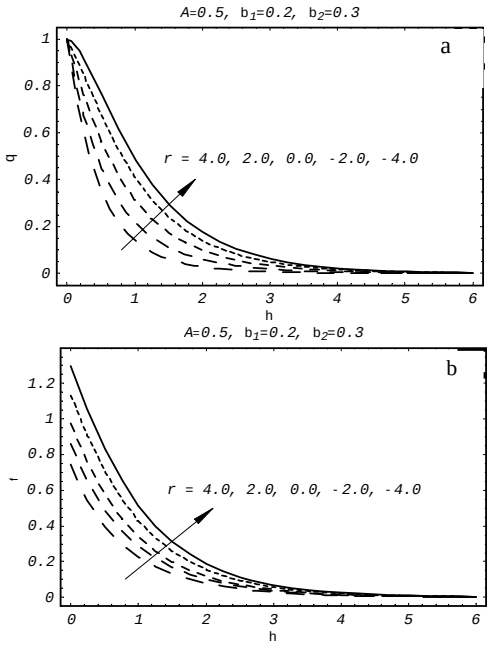

Fig. 6. Influence of r on the temperature, (a) CT case (b) CH case.

The effect of power indices r and s on the temperature profiles are seen through Figs. 6 and 7. It can be seen that the indices r and s have similar effect on the temperature profiles. It is observed that both decrease the temperature and thermal boundary layer thickness. Fig. 8 shows the effects of the heat source/sink parameter β on the temperature profiles $\theta(\eta)$ and $\phi(\eta)$. As expected, the temperature increases with increasing heat source $\beta > 0$ and decreases in the case of heat sink $\beta < 0$. The behavior of Prandtl number Pr on the temperature is shown in Fig. 9. The temperature decreases with an increase in Prandtl number which implies that the thermal boundary layer becomes thinner with large Prandtl number.

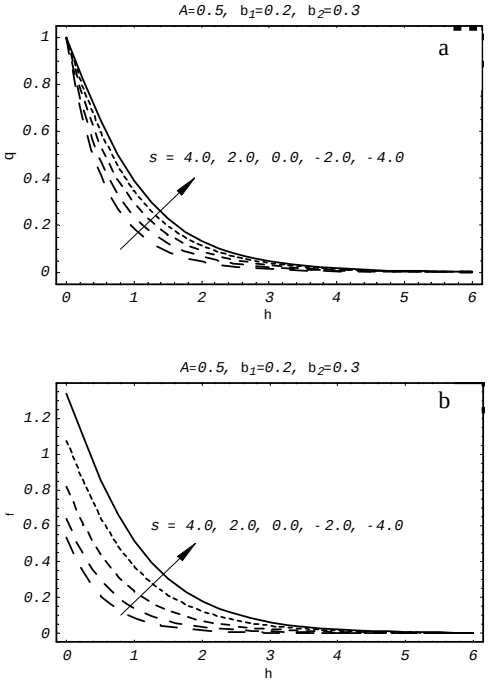

Fig. 7. Influence of s on the temperature, (a) CT case (b) CH case.

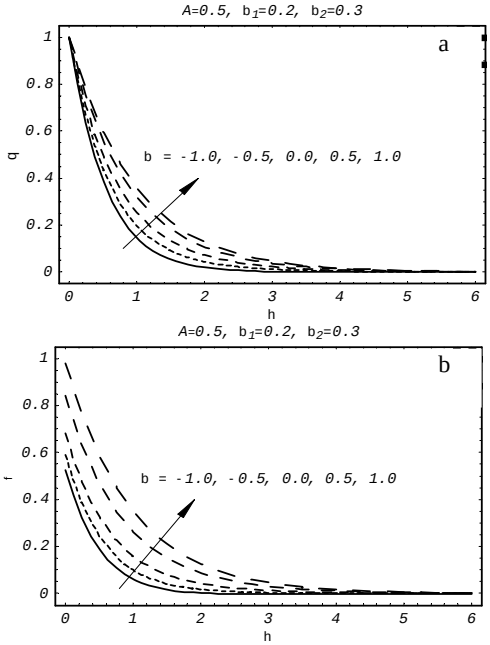

Fig. 8. Influence of β on the temperature, (a) CT case (b) CH case.

Table 2 provides a comparison for velocity fields in the special case when $\beta_1 = \beta_2 = A = 0$ and found in excellent agreement with Shehzad *et al*. (2013) and Khan *et al*. (2014). The comparison of $\theta'(0)$ and $\phi(0)$ for different values of Pr and β when $\beta_1 = \beta_2 = 0$, $r = s = 1$ and $\alpha = 0.5$ is presented

Table 2 Comparison of results for velocity fields for different values of α when $\beta_1 = \beta_2 = A = 0$ are fixed

α	Shehzad *et al*. (2013) Exact Sol.		Khan *et al*. (2014) HAM Sol.		Present result	
	$-f''(0)$	$-g''(0)$	$-f''(0)$	$-g''(0)$	$-f''(0)$	$-g''(0)$
0.0	1.0	0.0	1.0	0.0	1.0	0.0
0.1	1.020259	0.066847	1.02026	0.06685	1.020260	0.066846
0.2	1.039495	0.148736	1.03949	0.14874	1.039496	0.148742
0.3	1.05794	0.243359	1.05795	0.24336	1.057953	0.243358
0.4	1.075788	0.349208	1.07578	0.34921	1.075786	0.349209
0.5	1.093095	0.465204	1.09309	0.46521	1.093093	0.465209
0.6	1.109946	0.590528	1.10994	0.59053	1.109945	0.590532
0.7	1.126397	0.724531	1.12639	0.72453	1.126394	0.724530
0.8	1.142488	0.866682	1.14249	0.86668	1.142489	0.866684
0.9	1.158253	1.016538	1.15826	1.016538	1.158261	1.016538
1.0	1.173720	1.173720	1.17372	1.173720	1.173723	1.173722

Table 3 Numerical values of $-\theta'(0)$ and $\phi(0)$ when $A = 0$, $\beta = \beta_1 = \beta_2 = 0, r = 1, s = 1$ and $\alpha = 0.5$

		$-\theta'(0)$ for CT			$\phi(0)$ for CH		
		$\beta = -0.2$	$\beta = 0$	$\beta = 0.2$	$\beta = -0.2$	$\beta = 0$	$\beta = 0.2$
Liu & Andersson (2008)	$Pr = 1$	1.348064	1.255781	1.148932	0.741805	0.796317	0.870355
Present		1.348068	1.255778	1.148933	0.741806	0.796318	0.870370
Liu & Andersson (2008)	$Pr = 5$	3.330392	3.170979	3.002380	0.300265	0.315360	0.333069
Present		3.330395	3.170981	3.002379	0.300259	0.315363	0.333072
Liu & Andersson (2008)	$Pr = 10$	4.812149	4.597141	4.371512	0.207807	0.217527	0.228754
Present		4.812151	4.597143	4.371514	0.207806	0.217531	0.228755

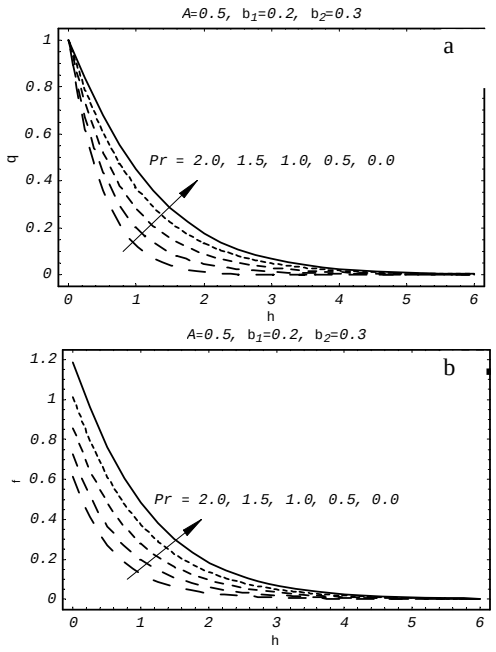

Fig. 9. Influence of Pr on the temperature, (a) CT case (b) CH case.

in table 3. From this table we examined that our series solutions have very good agreement with the previously obtained results. Table 4 gives the numerical values of local Nusselt number $-\theta'(0)$ for different values of Pr, α, β, A, r and s in both viscous and Oldroyd-B fluids. We observe that the values of local Nusselt number for viscous fluid case are quantitatively smaller in comparison to the Oldroyd-B fluid. It is also observed that an increase in the value of unsteadiness parameter A also increase the Nusselt number.

6. CONCLUDING REMARKS

The three-dimensional unsteady flow and heat transfer characteristics of an Oldroyd-B fluid due to an unsteady bidirectional stretching sheet is investigated in this paper. For the heat transfer analysis the heating process of (i) the constant temperature (CT) and (ii) the constant heat flux (CH) are taken in to account. The convergence of the developed series solution is explicitly discussed. The main findings of the present study are

- Temperature profiles $\theta(\eta)$ and $\phi(\eta)$ are the decreasing function of time dependent parameter A.
- The Deborah numbers β_1 and β_2 behaves quite oppositely on both the temperature profiles $\theta(\eta)$ and $\phi(\eta)$.
- A rise in Deborah number β_2 decrease the temperatures $\theta(\eta)$ and $\phi(\eta)$ and thermal boundary layer thickness.
- The numerical values of local Nusselt number for an Oldroyd-B fluid are larger than the viscous fluid.
- The temperature profile $\theta(\eta)$ and $\phi(\eta)$ are the decreasing function of Prandtl number.

Table 4 Numerical values of local Nusselt number $-\theta'(0)$ for different values of $Pr, \alpha, \beta, A, r, s, \beta_1, \beta_2$

α	Pr	A	β	r	s	$\beta_1 = \beta_2 = 0.0$	$\beta_1 = \beta_2 = 0.3$
0.25	1.0	0.5	0.0	0.0	0.0	1.069386	1.072114
0.50						1.108350	1.111716
0.75						1.158753	1.162966
0.50	0.5					0.739980	0.741497
	1.5					1.459927	1.465274
	1.0	0.0				0.716953	0.721059
		1.0				1.448419	1.450931
		0.5	-0.2			1.207769	1.210970
			0.2			0.997745	1.001277
			0.0	-2.0		0.340102	0.336027
				2.0		1.663113	1.670415
				0.0	-2.0	0.746805	0.748907
					2.0	1.412769	1.418924

- For $A = 0$, the steady flow situations will be obtained.
- For $\beta_1 = \beta_2 = 0$, the result for viscous fluid can be recovered.

ACKNOWLEDGMENT

Authors acknowledge the support provided by Higher Education Commission (HEC) of Pakistan. One of the authors M. Sajid acknowledges the support provided by AS-ICTP.

REFERENCES

Ahmad, I. (2013). On unsteady boundary layer flow of a second grade fluid over a stretching sheet. *Add. Theor. Appl. Mech.* 6, 695-105.

Ahmad, I., M. Ahmad and M. Sajid (2014). Heat transfer analysis of MHD flow due to unsteady bidirectional stretching sheet through porous space. *Ther. Sci*.

Ahmad, I., M. Ahmed, Z. Abbas and M. Sajid (2011). Hydromagnetic flow and heat transfer over a bidirectional stretching surface in a porous medium. *Ther. Sci.* 15, 205-220.

Ariel, P. D. (2003). Generalized three dimensional flow due to stretching surface, *Z. Angew. Math. Mech.* 83, 844-852.

Awais, M., T. Hayat, A. Alsaedi and S. Asghar (2014). Time-dependent three-dimensional boundary layer flow of a Maxwell fluid. *Comput. Fluids*. 91, 21–27.

Crane, L. J. (1970). Flow past a stretching plate. *Z. Angew Math. Phys.* 21, 645–647.

Haitao, Q. and X. Mingyu (2009). Some unsteady unidirectional flows of a generalized Oldroyd-B fluid with fractional derivative. *Appl. Math. Mod.* 33, 4184–4191.

Harris, J. (1977). *Rheology and Non-Newtonian Flow.* Longman, London.

Hayat, T. and A. Alsaedi (2011). On thermal radiation and Joule heating effects on MHD flow of an Oldroyd-B fluid with thermophoresis. *Arb. J. Sci. Eng.* 36, 1113–1124.

Hayat, T., M. Hussain, A. Alsaeedi, S. A. Shehzad and G. Q. Chen (2015). Flow of Power-law nanofluid over a stretching surface with Newtonian heating. *J. Appl. fluid Mech.*, 8, 273-280.

Hayat, T., M. Mustafa and A. A. Hendi (2011). Time dependent three dimensional flow and mass transfer of elastico-viscous fluid over unsteady stretching sheet. *App. Math. Mech.* 32, 167-178.

Hayat, T., S. A. Shehzad, S. A. Mezel and A. Alsaedi (2014). Three dimensional flow of an Oldroyd-B fluid over a bidirectional stretching surface with prescribed surface temperature and prescribed surface heat flux. *J. Hyrol. Hydromech.* 62, 117-125.

Hayat, T., S. A. Shehzad., M. Mustafa and A. A. Hendi (2012). MHD flow of an Oldroyd-B fluid through a porous channel. *Int. J. Chem. Reactor Eng.* 10, 1542-6580.

Hayat, T., T. Muhammad, S. A. Shehzad and A. Alsaedi (2015). Similarity solution to three dimensional boundary flow of second grade nanofluid past a stretching surface with thermal radiation and heat source/sink. *AIP Adv.,* 5, 017107.

Jamil, M., C. Fetecau and M. Imran (2011). Unsteady helical flows of Oldroyd-B fluids. *Commun. Nonlinear Sci. Numer. Simul.* 16, 1378–138.

Khan, W. A., M. Khan and R. Malik (2014). Three-dimensional flow of an Oldroyd-B nanofluid towards stretching surface with heat generation/absorption. *PLoS ONE* 9, e105107.

Liao, S. J. (1992). *The proposed homotopy analysis method for the solution of nonlinear problems*. PhD Thesis, Shangai Jiao Tong University.

Liao, S. J. (2003). *Beyond perturbation: Introduction to Homotopy Analysis Method.* Chapman & Hall, CRC Press, Boca Raton.

Liu, I. C. and H. I. Andersson (2008). Heat transfer

over a bidirectional stretching sheet with variable thermal conditions. *Int. J. Heat Mass Transf.* 51, 4018-4024.

Liu, Y., L. Zheng and X. Zhang (2011). Unsteady MHD Couette flow of a generalized Oldroyd-B fluid with fractional derivative. *Comput. Math. Appl.* 61, 443–450.

Sajid, M., Z. Abbas, T. Javed and N. Ali (2010). Boundary layer flow of an Oldroyd-B fluid in the region of stagnation point over a stretching sheet. *Can. J. Phys.* 88, 635–640.

Shehzad, S. A., A. Alsaedi, T. Hayat and M. S. Alhuthali (2013). Three dimensional flow of an Olroyd-B fluid with variable thermal conductivity and heat generation/absorption. *PLoS ONE* 8, e78240.

Turkyilmazoglu, M. (2012). Solution of the Thomas-Fermi equation with a convergent approach, *Commun. Nonlinear Sci. Numer. Simul.* 17, 4097-4103.

Wang, C. Y. (1989). The three dimensional flow due to stretching surface. *Phys. Fluids* 27, 1915-1917.

Xu, H., S. J. Liao and I. Pop (2007). Series solutions of unsteady three dimensional MHD flow and heat transfer in the boundary layer over an impulsively stretching plate. *Eur. J. Mech-B* 26, 15-2.